Biodegradable Intraprostatic Doxorubicin Implants

Submitted: March 14, 2007; Accepted: May 17, 2007; Published: June 29, 2007

Ronnie Ortiz,[1,2] Jessie L-S. Au,[1,3] Ze Lu,[1,4] Yuebo Gan,[1] and M. Guillaume Wientjes[1,3]

[1]College of Pharmacy, Ohio State University, Columbus, OH
[2]Current address: 3M Drug Delivery Systems, St Paul, MN
[3]James Cancer Hospital and Solove Research Institute, Ohio State University, Columbus, OH
[4]Current address: Optimum Therapeutics LLC, Columbus, OH

Abstract

Systemic chemotherapy is not effective in the treatment of prostate-confined cancer. We developed biodegradable, doxorubicin-loaded cylinders for intraprostatic implantation and evaluated the feasibility of using regional intraprostatic drug therapy to treat prostate-confined cancer. Cylinders were prepared using poly(lactide-co-glycolide) (PLG) or PLG copolymers. The in vitro and in vivo drug release, intraprostatic pharmacokinetics, and histopathology in dogs implanted with the cylinders were studied. The doxorubicin-loaded cylinders made of PLG polymers of 7.9 to 54 kDa molecular weight (MW) had a diameter of ~800 μm, drug loading of 10% to 30% (wt/wt), and even distribution of crystalline drug throughout the matrix. Burst release varied from 3% to 73%, and 7-day cumulative release from 4% to 90%. Decreasing polymer MW and increasing drug loading were associated with higher initial burst release and overall release rates. The in vivo drug release from cylinders (33-kDa PLG, 30% drug loading) in dog prostates was rapid (~80% in 48 hours). Spatial drug distribution, visualized using confocal fluorescence microscopy, showed high concentrations confined to the lobule containing the implant (referred to as the implanted lobule), with steep concentration gradients over the septa separating the lobules. Concentrations in the implanted lobule were about 8 times higher than concentrations delivered by an intravenous injection. The implants caused necrotic cell death in the implanted lobule, without damage to prostatic nerve bundles or the urethra. These results indicate the feasibility of using biodegradable PLG cylinders as intraprostatic implants to selectively deliver high drug concentrations to prostate tissue.

Keywords: PLG, doxorubicin, prostate delivery, controlled release, biodegradable implants

Introduction

Prostate cancer is the most common cancer and the second-leading cause of cancer death among American men; it accounts for ~11% of male cancer-related deaths.[1] Over the last decade, the availability of new screening techniques and the increased public awareness of the need for early testing have led to an increased incidence of localized disease (~80%) at diagnosis.[2] Therefore, effective treatment of localized disease has become increasingly important.

Radical prostatectomy has been the standard of treatment, offering the potential for tumor eradication and improved overall and disease-specific survival[3] but also causing complications, including incontinence in 5% to 31% and impotence in 18% to 89% of patients.[4] Radiotherapy and cryotherapy are less invasive but also cause impotence and incontinence. Because of the slow growth rate and late onset of prostate cancer, watchful waiting is another viable treatment option, currently recommended for older men with well-differentiated cancer.[4] Watchful waiting is associated with a higher quality of life compared with the invasive treatments but carries the risk of not treating a disease that can become metastatic and symptomatic.[5]

Systemic chemotherapy with cytotoxic drugs has been used to treat advanced, hormone-refractory prostate cancer but is seldom used to treat localized disease.[4] Our laboratory has shown that the effective doxorubicin concentrations in human prostate tumor histocultures far exceed the clinically achievable plasma concentrations delivered by intravenous administration (ie, 2 μM or 3.4 μg/mL vs <200 nM or 345 ng/mL).[6,7] Regional chemotherapy, which has been used clinically to treat other types of cancer, including bladder, skin, ovarian, colon, brain, and pancreatic cancer,[8-18] is an alternative approach to delivering high drug concentrations to the prostate.

Several properties of the prostate make it an ideal candidate for regional therapy. It is a small and encapsulated organ; these properties enable the achievement of high local drug concentrations while limiting unwanted side effects in extracapsular tissues. The blood perfusion rate to the prostate is relatively slow (ie, 16 mL/min/100 g[19]) compared with that of major organs such as the liver and the kidney.[20] This, in turn, limits the drug removal via the capillaries. In addition, the glandular prostate is composed of a relatively small number of the anatomical structures called lobules, ~15 in the dog and 20 to 70 in humans.[21] These cone-shaped structures are widest at the prostatic capsule and narrow as they approach the

Corresponding Author: M. Guillaume Wientjes, College of Pharmacy, 500 West 12th Avenue, Columbus, OH 43210. Tel: (614) 292-6488; Fax: (614) 688-3223; E-mail: wientjes.1@osu.edu

urethra. Acinar fluid formed in the lobule is emptied into the urethra through connecting ducts, creating a convective flow that can facilitate drug transport. This convection-facilitated transport is supported by our previous finding that prostate tissue penetration for the intraprostatic injection is >1 cm,[21] more than 3 times greater than the typical penetration distance mediated by diffusion alone, <0.3 cm.[22]

The lack of an important physiological function of the prostate's glandular tissue in men who are at the older age associated with a higher incidence of prostate cancer suggests that eliminating the normal, noncancerous prostate cells is not likely to result in unacceptable toxicity; this is supported by the generally accepted radical prostatectomy approach, where the tumor and normal tissues are simultaneously removed. Furthermore, relatively noninvasive technologies for reaching the prostate, for instance, transurethral and transrectal biopsies and resection, are well developed. The common use of brachytherapy, or direct placement of radioactive beads in the prostate, also supports intraprostatic implants as a viable alternative modality. The attractiveness of the prostate for regional chemotherapy delivery is elegantly presented in a recent review.[23] However, to our knowledge, no intraprostatic drug implants have been attempted.

For regional chemotherapy in prostate cancer to succeed, the drug should be released from the formulation in sufficient concentrations to produce appreciable antitumor activity in the localized tumors while limiting the drug absorption into the systemic circulation. Our previous studies established that densely packed epithelial tumor cells form a barrier to drug transport and that apoptosis-inducing treatments, by reducing the density, promote drug transport in tumor explants.[24] The time window for enhancing drug transport is between ~16 and 96 hours after the initial apoptotic insult. Based on this finding and on the pharmacodynamics of doxorubicin in prostate tumor explants,[7] we elected to develop formulations that provided rapid drug release in vivo, that is, complete release in no more than 4 days. A biodegradable formulation was preferred, to avoid the need for surgical removal. Based on these considerations, we elected to use poly(lactide-co-glycolide)–based (PLG-based) formulations, as PLG formulations are available with a wide range of compositions, molecular weights (MWs), and drug release rates[25]; have been used for regional chemotherapy applications[26,27]; and are approved by the US Food and Drug Administration for human use.[28-30] We chose doxorubicin because (1) its fluorescent properties enabled visualization of the spatial drug distribution, (2) it has activity against prostate cancer, (3) its high potency reduces the requirement of drug loading, and (4) it does not require metabolic activation.

The 2 goals of the present study were to develop biodegradable, doxorubicin-loaded cylinders and to evaluate the feasibility of using these cylinders as intraprostatic implants in dogs. The dog model was selected because of the anatomic similarities between dog and human prostates.[31]

Materials and Methods

Chemicals and Reagents

Doxorubicin hydrochloride was purchased from Hande Tech (Houston, TX), PLG (inherent viscosities of 0.18-0.63 dL/g, copolymer ratio of 50:50) from Birmingham Polymers (Birmingham, AL), and silicon tubing (inner diameter [ID] of 1/32″ or 794 μm, wall thickness of 1/32″) from Manostat (Barrington, IL). All other chemicals were of at least analytical grade, purchased from commercial suppliers, and used as received.

Preparation of Doxorubicin Cylinders

Cylinders were formed using a modified polymer extrusion technique.[32] Drug loading was varied between 10% and 30% (wt/wt). The MWs of PLG were 7.9, 9.4, 33, and 54 kDa. PLG of <10 kDa was not endcapped, while the higher-MW polymers were endcapped with an ester group. Acetone (130-460 μL), PLG (230 mg), and doxorubicin hydrochloride (26-100 mg) were mixed and stored overnight at 4°C. The viscous paste was transferred into a 3-mL syringe attached to silastic tubing (ID 1/32″) via a 0.5 in 18 gauge Luer stub adapter and was extruded into the tubing using a Harvard Infusion Pump (South Natick, MA) at a rate of 20 μL/min. After the tubing ends were clipped with binder clips, the cylinders were dried, allowed to cool to room temperature, and stored under vacuum in the silastic tubing. Cylinders were removed from the tubing and sterilized using gamma radiation (25 kGy) before in vivo use. The above procedures resulted in cylinders with cross-sectional diameters of 800 μm. For implantation in animals, the cylinders were cut to a length of 8 mm.

Scanning Electron and Confocal Microscopy

Cylinders were sectioned using a cryotome (Microm 500 Cryostat, Carl Zeiss, Inc, Thornwood, NY). For scanning electron microscopy (SEM), cross-sections and longitudinal sections were sputter-coated with gold in three 30-second intervals at 7 mA, and images were captured using a Philips XL-30 SEM (Philips, Eindoven, The Netherlands) at an accelerating potential of 10 keV. For studying doxorubicin distribution within the cylinders, cross-sections were placed on glass slides and analyzed using a laser confocal microscope equipped with an argon-krypton laser with excitation and emission wavelengths of 488 and 515 nm (BIO-RAD 600, Hercules, CA).

Characterization of Doxorubicin Cylinders

The glass transition temperature (T_g) of PLG was determined using a differential scanning calorimeter (Perkin-Elmer DSC 7, Norwalk, CT) calibrated with an indium standard. Samples (10-15 mg) were sealed in aluminum pans and scanned from 20°C to 80°C at a rate of 5°C/min under nitrogen purge. All thermograms were obtained from the first heating cycle to optimize the characterization of drug-polymer interaction in the cylinders.

SEM photographs of doxorubicin cylinders were used to determine the sizes of (1) doxorubicin crystals in cylinders prior to drug release, and (2) the pores within and on the surface of cylinders after drug release. At least 50 pores were measured for each sample.

In Vitro Doxorubicin Stability and Release From Cylinders

Sections of doxorubicin-loaded PLG cylinders (7-9 mm length, weighing 3-5 mg) were mixed with 5 mL Tris buffer (30 mM Tris HCl, 150 mM NaCl, 0.02% wt/vol Tween 80, pH 7.4) in an orbital shaker maintained at 125 rpm and 37°C. Release buffer samples were withdrawn at predetermined intervals and replaced with equal volumes of fresh buffer. Sink conditions, where doxorubicin concentrations in the release medium were below 10% of its aqueous solubility (2.1 mg/mL), were maintained at all times. The release buffer samples were directly analyzed for UV absorption at 490 nm. A 5-point standard curve was constructed and was linear from 1 to 200 μg/mL ($r^2 > 0.999$).

After the release study was complete, the cylinders were collected, flash-frozen, lyophilized, and dissolved in ~200 volumes of 80% acetonitrile in water. The amount of residual doxorubicin and its degradation products in the mixture was analyzed by high-performance liquid chromatography (HPLC) and used to calculate the ratio of unchanged and degraded drug and the mass balance. The HPLC system consisted of a Hitachi Intelligent Autosampler (Hitachi, Japan), a Waters 515 pump (Milford, MA), a Waters 470 fluorescence detector (excitation: 480 nm, emission: 550 nm), and a PerkinElmer Pecosphere C_{18} column (3 μm particle size, 83 × 4.6 mm). The mobile phase was a 75:25 mixture of 20 mM potassium dihydrogen phosphate (pH 3.0) and acetonitrile, delivered at a flow rate of 0.8 mL/min. The concentration of doxorubicin in the sample was determined using a standard curve that was linear between 1 ng/mL and 1 μg/mL ($r^2 > 0.99$).

Animal Protocol

Male beagle dogs (10-13 kg) were cared for in accordance with the *Guide for the Care and Use of Laboratory Animals*.[33] Animals received a stool softener and were fasted overnight. Anesthesia was induced with ketamine-xylazine and maintained with isoflurane, the residual stool was vacated, and an 8551 transrectal ultrasound probe (B&K Instruments, North Billerica, MA) was used to image the prostate and guide the implantation needle. An x-ray contrasting agent was injected into the urinary catheter so that the position of the urethra and bladder could be seen under fluoroscopy. A prostate seeding needle (18 gauge, 20 cm in length; Mick Radio-Nuclear, Bronx, NY) was then inserted parallel to the urethra under ultrasound guidance. The needle stylet was removed, and a cylinder was advanced through the needle sheath and inserted into the prostate. Each cylinder contained ~1.6 mg doxorubicin. Plasma samples were obtained throughout the experimentation. At 2.5, 5, 24, and 48 hours, dogs were euthanized by pentobarbital overdose. Prostates were excised, sliced in ~5-mm-thick sections (5 segments per prostate) using a cryotome blade, and flash-frozen.

Intraprostatic and Plasma Pharmacokinetics of Doxorubicin

Prostate tissues were analyzed using 2 methods. Confocal fluorescence microscopy was used to monitor the spatial distribution and distribution kinetics within a prostate at the early time points, when drug concentrations were sufficiently high. The frozen prostate tissue slices were cryosectioned into 10-μm sections using a Carl Zeiss Microm 500 cryostat. The sections were placed on glass slides and studied using a Meridian Instruments ACAS 570 (Okemos, MI) confocal fluorescence microscope. The excitation was with the 514-nm line of a 2-mW argon ion laser, and the emission at 575 nm (±12.5 nm) was recorded by a photomultiplier tube and digitized by a 12-bit microcomputer to produce pseudo-color images of fluorescence, captured with an Olympus 20X dry lens (Center Valley, PA), a 10-μm scanning step, and a pinhole setting of 1600 μm. Pixel intensity analysis was performed using Optimas Image Analysis software (Media Cybernetics, Silver Spring, MD). Fluorescent intensities obtained from the ACAS 570 were converted to a linear gray scale value using Optimas software. The doxorubicin-derived fluorescence intensity was corrected for background tissue fluorescence obtained using blank prostate cryosections. The linearity of the background-corrected pixel intensities with concentration was confirmed by comparing the tissue-average pixels (intensity over entire section) to the results obtained from HPLC analysis of tissue segments; the 2 measurements were highly correlated ($R^2 = 0.96$, in 6 tissue specimens containing 8-360 μg/g doxorubicin).

The second analysis used HPLC. Frozen, 5-mm-thick prostate tissue slices were further sectioned into multiple samples using a hollow boring tool (6.2 mm diameter). The first

sample contained the visible cylinder or, when the cylinder was not visible (eg, at later time points), the red-colored area (indicating location of doxorubicin). Additional samples located at successively longer distances away from the cylinder were obtained. After the visible implant material was carefully removed, a sample was weighed, extracted, and analyzed for doxorubicin using HPLC as described above. The limit of quantitation for the ~150 mg tissue specimens was 0.1 μg/g.

Plasma samples were extracted with methylene chloride using epirubicin as the internal standard, as previously described.[34] The lower detection limit for plasma was 1 ng/mL.

Histopathologic Evaluation

For histopathologic evaluation, dogs were implanted with doxorubicin-containing cylinders or blank PLG cylinders. Prostates were harvested at different time points up to 3 months after implantation and were prepared for microscopic evaluation. About half of the prostates were flash-frozen and cryosectioned in 10-μm sections throughout the prostate. The frozen sections were stained with hematoxylin and eosin. The other prostates were gross-sectioned into 5-mm-thick slices, formalin fixed, and paraffin embedded. Microscopy sections of 5 μm thickness were placed on glass slides and stained with hematoxylin and eosin. Serial sections of each prostate were evaluated under bright-field microscopy for histopathologic changes induced by the implants, including localized tissue damage, inflammation, wound healing response, and integrity of the prostatic urethra, prostatic capsule, and periprostatic nerve bundles.

RESULTS

Cylinder Morphology and Properties

Table 1 summarizes the properties of doxorubicin-loaded PLG cylinders consisting of copolymers with varying MWs and drug loading. The cylinder diameter (794 μm) was selected so that a cylinder could pass through an 18-gauge implantation needle (ID 840 μm). The glass transition temperature, T_g, when PLG changes from a glasslike state to a rubberlike state increased with the MW of PLG (eg, <37°C for <10 kDa to >40°C for 33-54 kDa) but was not affected by the extent of drug loading (eg, no differences for 0% or 30% loading).

Figures 1A and 1B show the SEM images of cross-sections and outer surfaces of doxorubicin-loaded cylinders before

Table 1. Effects of Cylinder Properties on Doxorubicin Release From PLG Cylinders*

PLG MW (kDa)	Drug Loading (%)	Initial Burst in 3 Hours (% of dose)	Cumulative Release Over 7 Days (% of dose)	Remaining in Cylinder After 7 Days (% of dose)	Residual Drug Loading (%)	Mass Balance (%)	Glass Transition Temperature (°C)
7.9	0	NA	NA	NA	NA	NA	28.5 ± 0.8
	10	4.2 ± 0.6	40.2 ± 3.5	55.7 ± 4.4	5.57	95.9 ± 4.0	29.2 ± 0.1
	20	15.5 ± 3.4	77.0 ± 1.4	19.6 ± 1.5	3.92	96.6 ± 1.1	29.2 ± 0.1
	30	73.4 ± 8.0	82.6 ± 1.0	14.7 ± 0.4	4.41	97.3 ± 1.5	29.7 ± 0.9
9.4	0	NA	NA	NA	NA	NA	32.3 ± 0.6
	10	4.2 ± 0.2	17.1 ± 8.0	76.8 ± 6.1	7.68	93.9 ± 7.7	33.4 ± 0.1
	20	15.5 ± 2.8	73.4 ± 4.6	25.9 ± 4.1	5.18	99.3 ± 2.0	33.7 ± 0.1
	30	62.5 ± 6.3	77.6 ± 1.6	18.3 ± 1.5	5.49	96.0 ± 2.2	33.2 ± 2.2
33	0	NA	NA	NA	NA	NA	39.6 ± 1.5
	10	3.3 ± 0.5	4.7 ± 0.8	93.3 ± 2.0	9.33	97.9 ± 3.0	42.7 ± 1.2
	20	14.1 ± 8.3	71.3 ± 11.7	25.7 ± 13.6	5.14	97.0 ± 0.8	43.5 ± 1.1
	30	42.6 ± 2.2	87.7 ± 1.8	7.9 ± 0.4	2.37	95.6 ± 2.4	43.0 ± 1.4
54	0	NA	NA	NA	NA	NA	44.3 ± 0.5
	10	2.8 ± 0.6	4.4 ± 0.8	90.9 ± 1.4	9.09	95.3 ± 1.5	47.8 ± 0.8
	20	10.8 ± 1.3	64.9 ± 2.0	29.4 ± 6.3	5.88	94.3 ± 1.3	46.8 ± 1.6
	30	28.4 ± 6.4	89.6 ± 8.0	8.5 ± 1.9	2.55	98.1 ± 8.2	46.6 ± 0.4

*Release of doxorubicin from cylinders into release buffer was monitored for initial burst release over 3 hours, cumulative release over 7 days, and residual amount in the cylinder after 7 days. Residual drug loading was calculated as the product of the initial loading and the fraction remaining in the cylinder after 7 days. Mass balance equals the sum of all 3 components. Glass transition temperatures (T_g) were determined using differential scanning calorimetry. Mean ± SD (n = 3). PLG indicates poly(lactide-co-glycolide); MW, molecular weight; NA, not applicable.

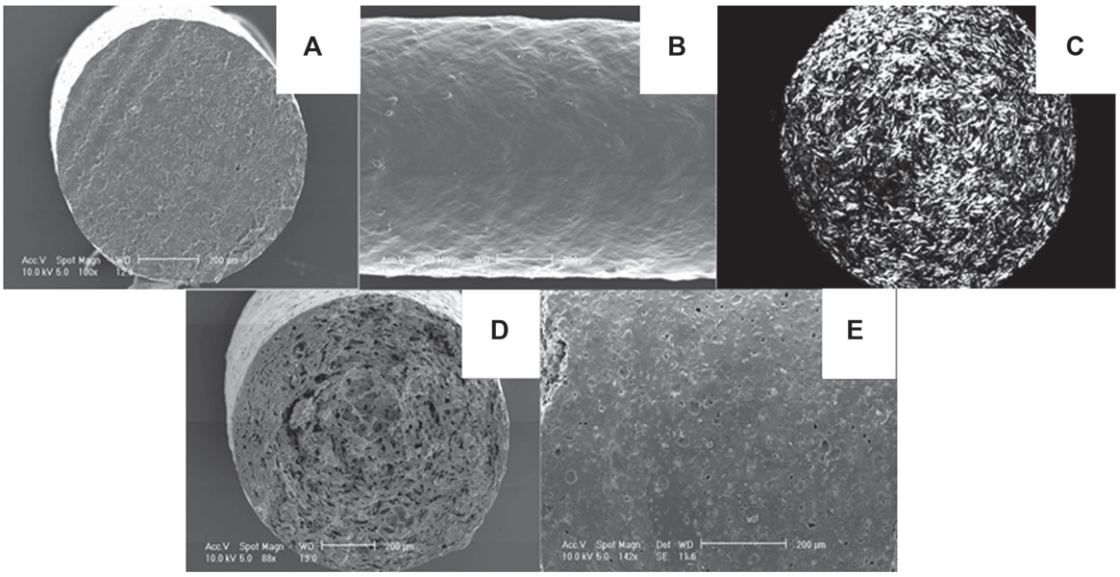

Figure 1. Cylinder morphology scanning electron microscopy of a cylinder made of 33-kDa PLG with 20% drug loading before (A and B) and after (D and E) incubation for 7 days in release medium (71% of the total drug load was released over this time period). Cross sections (A, C, D) and outer surfaces (B, E) of cylinders are shown. Figure 1C shows the even distribution of doxorubicin throughout the poly(lactide-co-glycolide) matrix. Doxorubicin-derived fluorescence is indicated by pixels with varying gray scale intensity, ranging from black for no doxorubicin to white for the highest doxorubicin concentration (×100). Note the appearance of pores within and on the outer surface of a cylinder after drug release.

drug release; cylinders showed solid and smooth outer surfaces and were void of internal air pockets. Figure 1C shows the homogeneous drug distribution throughout the PLG matrix. Figures 1D and 1E show the cylinder morphology after drug release, with channels and pores appearing on both the inside matrix and the outer surface. The mean pore diameter on the outside surface was 7.4 ± 2.2 μm (mean ± SD of 50 determinations), or within 20% of the mean diameter of 8.9 ± 1.9 μm of the doxorubicin hydrochloride crystals used to prepare the cylinders.

Effects of Cylinder Properties on In Vitro Drug Release

The initial burst release within the first 3 hours and the cumulative release over 7 days were affected by the MW of PLG and drug loading (Table 1). The initial burst drug release showed a 26-fold variation (Figure 2A). The highest release of >70% was observed for cylinders with the smallest PLG (7.9 kDa) and the highest drug loading (30%), while the lowest burst release (<3%) was observed for cylinders with the largest PLG (54 kDa) and the lowest drug loading (10%). For the cumulative drug release over 7 days, cylinders with low-MW PLG (7.9 and 9.4 kDa) showed a more rapid release compared with those with higher-MW PLG, irrespective of the drug loading (Figure 2B). But the greatest difference was observed at the lowest drug loading: the smaller PLG showed a second phase of rapid release of >10% of the dose starting on day 3 or 5; this was absent for the larger PLG.

In general, drug loading had a greater effect on the extent of cumulative drug release than did the size of PLG, although the difference was more pronounced for cylinders with larger PLG. For example, increasing the drug loading from 10% to 30% resulted in a 2-fold higher release (from 40% to 83%) from cylinders with smaller PLG (7.9 kDa), compared with a 20-fold higher release (from 4.4% to 90%) from cylinders with larger PLG (54 kDa).

During the in vitro release study over 7 days, cylinders with smaller PLG (<10 kDa) and lower drug loading (10%) lost their cylindrical shape and compacted into a sphere. In contrast, cylinders prepared with the same polymers but higher drug loading (>20%) maintained their original cylindrical shape.

HPLC analysis of the extracts of cylinders recovered after the 7-day release study showed only doxorubicin and no degradation products such as doxorubicinol and doxorubicinone, which are the predominant degradation products at pH < 3.[35] The amount of unchanged doxorubicin recovered from cylinder extracts ranged from ~8% to 91% and, as would be expected, was inversely correlated with the cumulative amount of drug recovered in the release medium. The sums of the dose fractions found in the release medium and the fraction in cylinder extracts represent over 96% of the drug loading (Table 1).

For all implants, irrespective of initial drug loading or polymer MW, the residual amount of doxorubicin after 7-day release ranged from 4% to 9%.

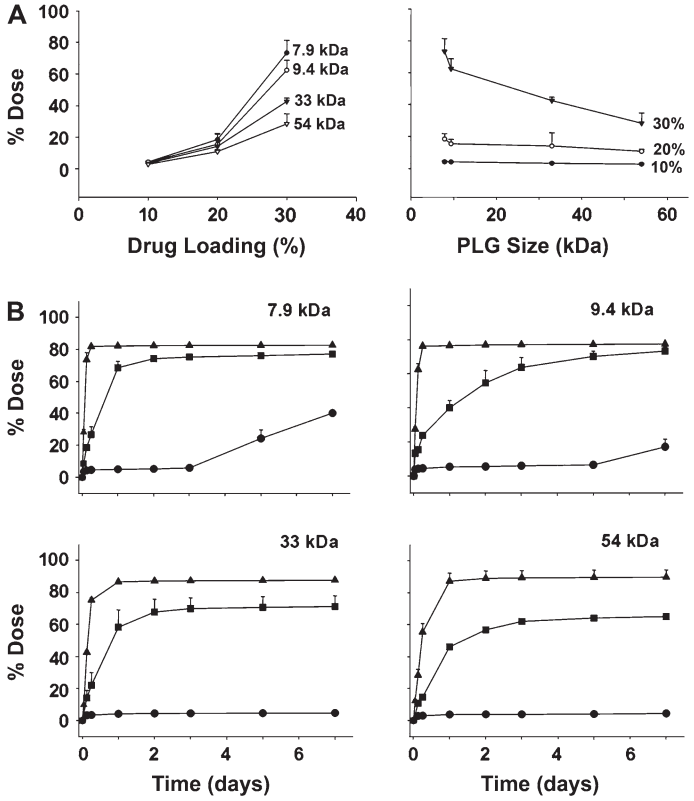

Figure 2. Effects of cylinder properties on drug release under in vitro conditions. Drug release experiments were conducted in an aqueous medium at 37°C. (A) Initial burst release within 3 hours. (B) Cumulative release over 7 days. Drug loading of 10% (●), 20% (■), or 30% (▲). Mean + SD of 3 experiments. PLG indicates poly(lactide-co-glycolide).

Selection of Doxorubicin-Loaded PLG Cylinders for In Vivo Evaluation

The desirable characteristics of cylinder implants for intraprostatic implantation are as follows. First, the drug release from cylinders should be such that pharmacologically active concentrations and exposure times are attained in prostate tissues. Based on our previous studies, the respective doxorubicin concentrations required to produce 50% cytostasis and cytotoxicity in human prostate tumor specimens are 1.8 and 59 μg/g for a 4-day exposure.[36] Hence, the selected cylinder should have a high drug loading, and the implanted cylinders should release the drug content within a similar time frame. Further, cylinders with a Tg above the body temperature are more rigid and easier to push through the implantation needle compared with cylinders with Tg below the body temperature. Smaller copolymers were preferred because of their slightly faster drug release. Based on these considerations, we selected the cylinder composed of 33-kDa PLG with a Tg of 40°C, 30% doxorubicin loading, and 88% release of the drug load over 7 days.

Fate of Doxorubicin-Loaded PLG Cylinders In Vivo

We monitored the degradation and drug release from cylinders after implantation in dog prostate. Intact cylinders were observed for up to 3 days, whereas fragments accompanied by discernable doxorubicin-derived fluorescence in adjacent tissues were observed for up to 11 days (not shown). Neither cylinder fragments nor doxorubicin fluorescence could be observed on day 28. These data confirm the biodegradable property of PLG.

Intraprostatic and Plasma Pharmacokinetics in Dogs Implanted With Doxorubicin Cylinders

Figure 3 shows the confocal fluorescence microscopy results. Changes in fluorescence intensity with respect to distance from the outer edge of an implant were measured in 4 perpendicular directions; the results for 2.5- and 24-hour samples are shown. For the 2.5-hour sample, the fluorescence intensity declined logarithmically with increasing distance away from the implant, with a 50% decline over 250 μm. This concentration gradient diminished over time, such that the 24-hour samples showed relatively constant fluorescence intensity in tissues throughout the lobule where the implant was situated. In all samples, the distribution of fluorescence signals was restricted to the implanted lobule. This was confirmed by microscopic observation showing that the sharp boundary of the fluorescence occurred at the septa separating the lobules.

For HPLC analysis, prostate tissue samples were separated into 4 categories corresponding to the distance from the implanted cylinder (Table 2). The HPLC measurements provided tissue concentrations and areas under the concentration-time curve (AUCs). The results showed that a mean AUC of greater than 6000 μg/g*hr could be achieved at a distance of less than 3 mm away from the cylinder, dropping off to 375 μg/g*hr at distances of 3 to 9 mm. In more than half of the cases, detectable drug concentrations were found in at least 1 tissue sample taken from above or below the implants (~14 mm away from the cylinder). Doxorubicin was not detectable (<0.1 μg/g) in 165 samples taken from the half of the prostate contralateral to the implantation site. Our previous studies in patient prostate tumor explants found that treatment with ~0.6 and ~60 μg/g doxorubicin for 96 hours (equivalent to ~60 and ~6000 μg/g*hr cumulative exposure) was sufficient to cause 50% cytostasis and 50% cell death, respectively.[7] Comparisons of the previous in vitro pharmacodynamic data with the current tissue concentration data suggest that cytocidal doxorubicin concentrations are achieved in the direct vicinity of the implants and cytostatic concentrations are achieved at distances of up to 14 mm away from the implants.

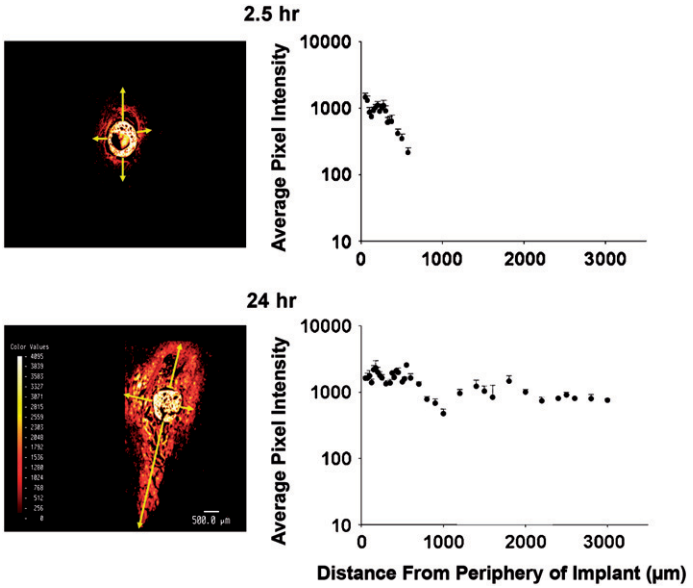

Figure 3. Spatial drug distribution in prostates: confocal fluorescence microscopy results. Dog prostates were harvested at the indicated time points, sliced in 5-mm-thick segments, and snap-frozen. Cryosections (10-mm thick) were analyzed using confocal fluorescence microscopy and image analysis. Left panels: micrographs showing the fluorescence signals. The cross-sections of implants are visible as high-intensity spherical areas. Note that the fluorescence intensity decreased with increasing distance from the implant. Also note that drug distribution was confined to the cone-shaped prostatic lobule where the cylinder resided, as indicated by the sharp boundary of fluorescence distribution coinciding with the lobular septa. Pixel intensities were converted to pseudocolors (see insert). Right panels: changes in pixel intensities with respect to distance from the periphery of the implant. To measure the spatial distribution, we selected 4 directions across the tissue plane (indicated by the yellow arrows) and measured the area-averaged pixel intensity for areas of 30 × 30 μm, beginning from the outer edge of the implant and following the direction of the arrows. A comparison of the concentration declines at 2.5 and 24 hours indicates that there was a diminished concentration gradient over time and that even distribution was achieved at 24 hours.

Tissue concentrations increased with time between 2.5 and 5 hours, followed by a decline of ~80% at 48 hours. This is consistent with the rapid in vitro drug release from 33-kDa PLG cylinders, where 85% of the drug load was released in 48 hours.

The extent of drug absorption into the systemic circulation was monitored by measuring the drug concentrations in plasma. In 6 dogs that received single cylinder implants (equivalent to a dose of ~1.6 mg), the plasma concentrations in 39 samples obtained from 5 minutes to 7 days after implantation were undetectable (<1 ng/mL). A single dog receiving 6 implants containing a total dose of 11.2 mg doxorubicin showed a maximal plasma concentration of ~6 ng/mL maintained from 10 to 60 minutes, declining to ~3 ng/mL at 90 minutes and to below 1 ng/mL at 150 minutes. These concentrations are less than 1% of the plasma concentrations observed after a clinical dose in human patients.[37]

Since prostate tumors metastasize to the iliac lymph nodes, doxorubicin concentrations in these lymph nodes were determined after cylinder implantation. No detectable concentrations were found in any of the 16 specimens.

Toxicity and Histopathologic Changes After Cylinder Implantation

The implantation of blank or doxorubicin-containing cylinders had no apparent effect on the prostatic urethra and surrounding tissue, the prostatic capsule and periprostatic nerve bundles, but produced a mild inflammatory response at the implantation site (presence of neutrophils as early as 2.5 hours and lymphocytes on days 4 and 7). No evidence of inflammation was observed by day 28. Implantation of doxorubicin-containing cylinders resulted in widespread cellular necrosis confined to the implanted lobules; necrosis was observed at 24 hours (Figure 4), was still present at day 4, began to diminish by day 7, and was replaced by atrophied lobules on day 28. In comparison, no cellular necrosis was observed in dogs receiving blank PLG cylinders. The animals showed no signs of discomfort after cylinder implantation.

Discussion

This report describes the development and the in vitro and in vivo characterization of biodegradable, doxorubicin-loaded PLG implants. The implants, with drug loading of up to 30%, could be readily placed in the prostate using an implantation needle under ultrasound guidance. The results in dogs indicate that intraprostatic implantation of these cylinders yielded therapeutic concentrations in prostate tissues adjacent to the implants (see below). The maximal tissue AUC of ~6000 μg/g*hr derived from an intraprostatic implant (containing 1.6 mg doxorubicin) was ~8 times the tissue AUC derived from an intravenous injection of the same dose (750 μg/g*hr[38]). This indicates a significant pharmacokinetic advantage for the intraprostatic implants.

Analysis of drug concentrations in the prostate using confocal fluorescence microscopy and HPLC indicate that drug distribution was confined to tissues within the prostatic lobule where the cylinder resided. The restricted, intralobular distribution is consistent with our previous observation with an intraprostatic doxorubicin infusion into a dog prostate.[21] The drug release and distribution was rapid, resulting in evenly distributed drug concentrations within the lobule after 24 hours. This may be due to the convective flow created by the acinar fluid flow (see Introduction). In our previous doxorubicin infusion study,[21]

Table 2. Doxorubicin Concentrations in Prostate Tissues After Implantation of PLG Cylinders*

Time (hr)	Doxorubicin (µg/g)		
	Category I <3 mm From Cylinder (# detectable/total)	**Category II <9 mm From Cylinder (# detectable/total)**	**Category III <14 mm From Cylinder (# detectable/total)**
2.5	173 ± 135 (5/5)	5.04 ± 3.73 (3/4)	4.41 ± 3.77 (3/4)
5	279 ± 349 (7/7)	8.82 ± 11.38 (2/4)	1.13 ± 1.96 (1/3)
24	113 ± 78 (7/7)	11.90 ± 12.08 (3/5)	3.94 ± 5.01 (2/3)
48	30 ± 20 (4/4)	1.02 ± 1.49 (2/3)	2.47 ± 3.49 (1/2)
AUC	6230 µg/g*hr	375 µg/g*hr	138 µg/g*hr

*At selected time points after cylinder implantation, dog prostates were harvested and sectioned in slices of 5 mm thickness, perpendicular to the direction of cylinder implantation. Tissue samples (6.2 mm diameter) were obtained. Category I samples contained tissues immediately surrounding the cylinder. Category II samples were located directly below or above Category I samples. Category III samples were located above or below Category II samples. In all 165 Category IV samples, which were located in the contralateral half of the prostate, doxorubicin concentrations were undetectable (<0.1 µg/g). Cylinder implant material was removed from the tissue specimen before concentration analysis. Mean ± SD of 3 dogs for the 2.5-, 5-, and 24-hour time points and 2 dogs for the 48-hour time point. The number of samples with detectable doxorubicin concentrations and the number of total samples are indicated in parentheses. AUC indicates area under the concentration-time curve from 0 to 48 hours, calculated using the trapezoidal rule.

an even distribution of drug concentrations in the lobule was observed after 2.5 hours. The more rapid distribution after infusion is likely due to the larger convective flow resulting from the infused fluid volume in addition to the acinar fluid production.

The current studies were performed in healthy dogs. The possibility that drug transport may be altered by tumors could not be ruled out and warrants further investigation.

Release Mechanism

The implants used in our study were PLG-based solid dispersion systems with doxorubicin loading of 10% and 30%. The release from the high drug-load cylinders (20% and 30% load) was more rapid compared with the release from the low (10%) drug-load cylinders (eg, 10 to 14 times faster initial burst over 3 hours). This is likely due to the difference in the pores within the cylinders created by the dissolution of doxorubicin crystals, with a greater porosity (and therefore a greater drug diffusivity) for the higher drug-load cylinders, as has been reported for biodegradable polymer implants used to treat gliomas.[22,39,40]

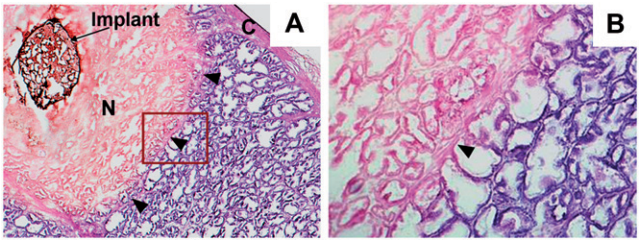

Figure 4. Widespread necrosis in implanted lobule. (A) Photomicrograph showing a cross-section of a dog prostate 24 hours after implantation of a doxorubicin-containing cylinder. Necrosis (N) was limited to the implanted lobule, with highly eosinophilic changes extending to the fibromuscular septa that define the implanted lobule (black arrowheads). No damage was seen in the prostatic capsule (C). Hematoxylin and eosin staining, ×25 magnification. (B) Area in Figure 4A outlined by dark red box in higher magnification (×100). Note the sharp demarcation between necrotic cells in the implanted lobule and normal-appearing cells in the adjacent lobule.

Suitability of PLG Copolymers as Matrix Materials

Previous implantable devices for doxorubicin delivery used glutaraldehyde cross-linked gelatin[41] and polyanhydride polymers.[40] One drawback of the gelatin formulation was that glutaraldehyde reacted with doxorubicin.[41] The anhydride pellets contained up to 5% doxorubicin dissolved in the matrix. The drug release from the anhydride formulation was sufficient to produce activity against rat gliomas but was considerably slower than the desired release for prostate tumors (<4 days). Our selection of PLG copolymer as the implant matrix material was in part based on its well-established biocompatibility and its wide acceptance for medical use (see Introduction). In addition, doxorubicin is stable in an acidic environment, with minimal hydrolytic degradation within a pH range of 3 to 6.5.[35,42] The microenvironment inside the PLG matrix is acidic, with a pH range of between 2 and 4.[43] The high stability of doxorubicin in PLG cylinders was confirmed by the nearly complete (96%) recovery and the absence of degradation products after 7 days.

Feasibility of Using the Implants

Whether drug-loaded implants can be used to treat prostate cancer depends on several factors. The first consideration is

whether the doxorubicin-loaded PLG implants deliver sufficient drug concentrations to attain meaningful antitumor activity. The results indicate that a single 0.8 mm × 8 mm implant containing 1.6 mg doxorubicin would yield an average tissue AUC of ~6000 μg/g*hr in tissues within 3 mm of the implant. This AUC is similar to the AUC that produced 50% cell death concentrations in human prostate tumors.[7] Hence, 1 implant provides a therapeutic concentration to ~400 mg of tissue. The second consideration is whether it is feasible to implant sufficient numbers of cylinders to deliver a therapeutic concentration to the entire prostate. We calculated that in order to provide sufficient AUC throughout an average human prostate with a 25-g glandular tissue weight, a total of 55 implants would be required. This is technically feasible in view of the practice of brachytherapy, where 80 to 110 seeds of radioactive iodine-125 or palladium-103 are typically implanted at points 1 cm apart in a single prostate.[44,45] The third consideration is the local and systemic toxicity of the implants. Systemic toxicity is unlikely as the corresponding total doxorubicin dose in 55 implants would be ~89 mg or 52 mg/m², which is below the recommended dose of 60 to 80 mg/m² for intravenous administration.[37,46] Hence, systemic absorption, even if it is complete and rapid, is not expected to result in significant systemic toxicity. The toxicity after single doxorubicin implants was limited to the implanted lobule, suggesting acceptable local toxicity, in agreement with the lack of serious toxicity in animals and humans receiving regional doxorubicin administration.[27,47] An example of a well-tolerated clinical use of local doxorubicin therapy is the treatment of superficial bladder cancer, where a dose of 50 to 150 mg is dispersed in a volume of 150 mL.[46] On the other hand, extravasation of anthracyclines and other chemotherapeutics has been associated with tissue necrosis.[48] Further development of intraprostatic doxorubicin implants should proceed with caution so that the potential local toxicity can be carefully controlled.

Conclusion

The present study demonstrates that implants of biodegradable, drug-loaded PLG cylinders can be used to deliver high drug concentrations in the prostate with comparatively low systemic concentrations. The study supports our contention that the prostate is a suitable organ for regional drug delivery approaches. Additional studies to integrate the pharmacodynamics of doxorubicin in prostate tumors into the design of the implants are warranted.

Acknowledgments

This study was supported in part by research grant R01CA74179 from the National Cancer Institute, US Department of Health and Human Services.

References

1. Pienta KJ, Smith DC. Advances in prostate cancer chemotherapy: a new era begins. *CA Cancer J Clin*. 2005;55:300-318.

2. Jemal A, Murray T, Samuels A, Ghafoor A, Ward E, Thun MJ. Cancer statistics, 2003. *CA Cancer J Clin*. 2003;53:5-26.

3. Bill-Axelson A, Holmberg L, Ruutu M, et al. Radical prostatectomy versus watchful waiting in early prostate cancer. *N Engl J Med*. 2005;352:1977-1984.

4. Bracarda S, de Cobelli O, Greco C, et al. Cancer of the prostate. *Crit Rev Oncol Hematol*. 2005;56:379-396.

5. Lu-Yao GL, Yao SL. Population-based study of long-term survival in patients with clinically localized prostate cancer. *Lancet*. 1997;349:906-910.

6. Chen CT, Gan Y, Au JL, Wientjes MG. Androgen-dependent and -independent human prostate xenograft tumors as models for drug activity evaluation. *Cancer Res*. 1998;58:2777-2783.

7. Chen CT, Au JL, Wientjes MG. Pharmacodynamics of doxorubicin in human prostate tumors. *Clin Cancer Res*. 1998;4:277-282.

8. Ikeda R, Chikazawa I, Kobayashi Y, et al. Prophylaxis of recurrence in superficial bladder carcinoma by intravesical chemotherapy—comparative study between instillation of combined double anticancer agents and single anticancer agent. *Gan To Kagaku Ryoho*. 1999;26:509-514.

9. Aigner KR, Gailhofer S, Kopp S. Regional versus systemic chemotherapy for advanced pancreatic cancer: a randomized study. *Hepatogastroenterology*. 1998;45:1125-1129.

10. Beger HG, Link KH, Gansauge F. Adjuvant regional chemotherapy in advanced pancreatic cancer: results of a prospective study. *Hepatogastroenterology*. 1998;45:638-643.

11. Firusian N, Dempke W. An early phase II study of intratumoral P-32 chromic phosphate injection therapy for patients with refractory solid tumors and solitary metastases. *Cancer*. 1999;85:980-987.

12. McClay EF, Howell SB. A review: intraperitoneal cisplatin in the management of patients with ovarian cancer. *Gynecol Oncol*. 1990;36:1-6.

13. Recio FO, Piver MS, Hempling RE, Driscoll DL. Five-year survival after second-line cisplatin-based intraperitoneal chemotherapy for advanced ovarian cancer. *Gynecol Oncol*. 1998;68:267-273.

14. Sandor V, Stark-Vancs V, Pearson D, et al. Phase II trial of chemotherapy alone for primary CNS and intraocular lymphoma. *J Clin Oncol*. 1998;16:3000-3006.

15. Orfanos CE, Zouboulis CC, Almond-Roesler B, Geilen CC. Current use and future potential role of retinoids in dermatology. *Drugs*. 1997;53:358-388.

16. Schneebaum S, Jr, Arnold MW, Jr, Staubus A, Jr, Young DC, Jr, Dummond D, Jr, Martin EW, Jr. Intraperitoneal hyperthermic perfusion with mitomycin C for colorectal cancer with peritoneal metastases. *Ann Surg Oncol*. 1996;3:44-50.

17. Ishikawa O, Ohigashi H, Imaoka S, et al. Regional chemotherapy to prevent hepatic metastasis after resection of pancreatic cancer. *Hepatogastroenterology*. 1997;44:1541-1546.

18. Link KH, Gansauge F, Gorich J, Leder GH, Rilinger N, Beger HG. Palliative and adjuvant regional chemotherapy in pancreatic cancer. *Eur J Surg Oncol*. 1997;23:409-414.

19. Inaba T. Quantitative measurements of prostatic blood flow and blood volume by positron emission tomography. *J Urol*. 1992; 148:1457-1460.

20. Davies B, Morris T. Physiological parameters in laboratory animals and humans. *Pharm Res*. 1993;10:1093-1095.

21. Wientjes MG, Zheng JH, Hu L, Gan Y, Au JL. Intraprostatic chemotherapy: distribution and transport mechanisms. *Clin Cancer Res*. 2005;11:4204-4211.

22. Fung LK, Shin M, Tyler B, Brem H, Saltzman WM. Chemotherapeutic drugs released from polymers: distribution of 1,3-bis(2-chloroethyl)-1-nitrosourea in the rat brain. *Pharm Res*. 1996;13:671-682.

23. Farokhzad OC, Dimitrakov JD, Karp JM, Khademhosseini A, Freeman MR, Langer R. Drug delivery systems in urology—getting "smarter." *Urology*. 2006;68:463-469.

24. Au JL, Jang SH, Zheng J, et al. Determinants of drug delivery and transport to solid tumors. *J Control Release*. 2001;74:31-46.

25. Piskin E. Biodegradable polymers as biomaterials. *J Biomater Sci Polym Ed*. 1995;6:775-795.

26. Yemisci M, Bozdag S, Cetin M, et al. Treatment of malignant gliomas with mitoxantrone-loaded poly (lactide-co-glycolide) microspheres. *Neurosurgery*. 2006;59:1296-1303.

27. Menei P, Montero-Menei C, Venier MC, Benoit JP. Drug delivery into the brain using poly(lactide-co-glycolide) microspheres. *Expert Opin Drug Deliv.* 2005;2:363-376.

28. Stoeckemann K, Sandow J. Effects of the luteinizing-hormone-releasing hormone (LHRH) antagonist ramorelix (hoe013) and the LHRH agonist buserelin on dimethylbenz anthracene-induced mammary carcinoma: studies with slow-release formulations. *J Cancer Res Clin Oncol*. 1993;119:457-462.

29. Santen RJ, Manni A, Harvey H. Gonadotropin releasing hormone (GnRH) analogs for the treatment of breast and prostatic carcinoma. *Breast Cancer Res Treat*. 1986;7:129-145.

30. Blom JH, Hirdes WH, Schroder FH, et al. Pharmacokinetics and endocrine effects of the LHR analogue buserelin after subcutaneous implantation of a slow release preparation in prostatic cancer patients. *Urol Res*. 1989;17:43-46.

31. Lowseth LA, Gerlach RF, Gillett NA, Muggenburg BA. Age-related changes in the prostate and testes of the beagle dog. *Vet Pathol*. 1990;27:347-353.

32. Zhou T, Lewis H, Foster RE, Schwendeman SP. Development of a multiple-drug delivery implant for intraocular management of proliferative vitreoretinopathy. *J Control Release*. 1998;55:281-295.

33. Institute of Laboratory Animal Resources (US). *Guide for the Care and Use of Laboratory Animals.* Washington, DC: National Academy Press; 1996.

34. Beijnen JH, Meenhorst PL, van Gijn R, Fromme M, Rosing H, Underberg WJ. HPLC determination of doxorubicin, doxorubicinol and four aglycone metabolites in plasma of AIDS patients. *J Pharm Biomed Anal*. 1991;9:995-1002.

35. Wassermann K, Bundgaard H. Kinetics of the acid-catalyzed hydrolysis of doxorubicin. *Int J Pharm*. 1983;14:73-78.

36. Chen CT, Au JL, Gan Y, Wientjes MG. Differential time dependency of antiproliferative and apoptotic effects of taxol in human prostate tumors. *Urol Oncol*. 1997;3:11-17.

37. Bugat R, Robert J, Herrera A, et al. Clinical and pharmacokinetic study of 96-h infusions of doxorubicin in advanced cancer patients. *Eur J Cancer Clin Oncol*. 1989;25:505-511.

38. Hu L, Au JL, Wientjes MG. Computational modeling to predict effect of treatment schedule on drug delivery to prostate in humans. *Clin Cancer Res*. 2007;13:1278-1287.

39. Brem H. Polymers to treat brain tumours. *Biomaterials*. 1990;11:699-701.

40. Lesniak MS, Upadhyay U, Goodwin R, Tyler B, Brem H. Local delivery of doxorubicin for the treatment of malignant brain tumors in rats. *Anticancer Res*. 2005;25:3825-3831.

41. Fan H, Dash AK. Effect of cross-linking on the in vitro release kinetics of doxorubicin from gelatin implants. *Int J Pharm*. 2001;213:103-116.

42. Vigevani A, Williamson M. Doxorubicin. In: Florey K, ed. *Analytical Profiles of Drug Substances.* New York, NY: Academic Press; 1980.

43. Shenderova A, Burke TG, Schwendeman SP. Stabilization of 10-hydroxycamptothecin in poly(lactide-co-glycolide) microsphere delivery vehicles. *Pharm Res*. 1997;14:1406-1414.

44. Sylvester J, Blasko JC, Grimm P, Ragde H. Interstitial implantation techniques in prostate cancer. *J Surg Oncol*. 1997;66:65-75.

45. Tapen EM, Blasko JC, Grimm PD, et al. Reduction of radioactive seed embolization to the lung following prostate brachytherapy. *Int J Radiol Oncol Biol Phys.* 1998;42:1063-1067.

46. Mosby's Drug Consult. doxorubicin. Available at: www.mdconsult.com. Accessed May 29, 2007.

47. Averbach A, Stuart OA, Chang D, Sugarbaker PH. Lattice intrahepatic doxorubicin with and without in-flow occlusion: a pharmacokinetic study of direct liver injection. *Eur J Surg Oncol*. 2000;26:73-79.

48. Schrijvers DL. Extravasation: a dreaded complication of chemotherapy. *Ann Oncol*. 2003;14:iii26-iii30.